An analytical study on the static vertical stiffness of wire rope isolators

***P.S. Balaji*[a]*, Leblouba Moussa*[b] *M.E. Rahman*[c#]*, Lau Hieng Ho*[d]**

[a,c,d]*School of Engineering and science, Curtin University Sarawak, Miri – 98009, Malaysia.*

[b]*University of Sharjah, Department of Civil & Environmental Engineering.*

Corresponding author:
Email address: merahman@curtin.edu.my
Tel: +60 85 443939 Ext : 3816 Fax: +60 85 443838

Abstract:

The vibrations due to earthquake ground motions or due to operations of heavy machineries, can affect the functionality of equipment and cause structural damages to the structures and surrounding equipment. The wire rope isolator (WRI), a type of passive isolator is known to be effective in isolating the vibrations and shock, can be used for vibration isolation of structures and equipment. The primary advantage of WRI is that, it can provide isolation in all three planes and in any orientation. The load-supporting capability of WRI is identified from the static stiffness in the loading direction. The static stiffness depends mainly on the geometrical and material properties of the WRI. The present work involves in the development of an analytical model for the static stiffness in the vertical direction using Castigliano's second theorem and validated with the experimental results obtained from the monotonic loading test. The flexural rigidity of the wire ropes required in the model was obtained from the transverse bending test. The analytical model is then used to perform a parametric analysis on the effects of wire rope diameter, width, height, and number of turns (loops) on the vertical stiffness. It is observed that the wire rope diameter influences the stiffness significantly more than the other geometric parameters. The developed model can be accurately used for the evaluation and design of wire rope isolators.

Keywords: Vibration, Isolation, Wire rope isolator, Vertical stiffness, Flexural rigidity.

1. Introduction

The vibrations from the sources such as earthquakes or due to operations of heavy machineries can affect the functionality of equipment and cause structural damages to the hosting structures. This signifies the application of vibration Isolators to isolate the system from the vibration environment [1-4]. Wire Rope Isolators (WRI), a type of passive isolators, known to be effective in isolating the vibration and shocks, can be used to protect the system [5, 6]. WRI is made up of wire rope held between a metal retainer either in a form of helical or arch and called helical WRI (Fig. 1(a)) or polycal WRI (Fig. 1(b)) respectively. The individual wire strands of the wire rope are in frictional contact and move relative to each other hence friction causes the dissipation of vibrational energy [5-7]. WRI has recently gained the attention among researchers and become subject of intense study. WRI has been extensively applied for shock and vibration isolation in military and industrial applications [2]. The primary advantage of WRI is their ability to provide isolation in three planes and in all the directions, due to which it can be mounted in any orientation to protect structures and equipment excited in any directions [5, 6].

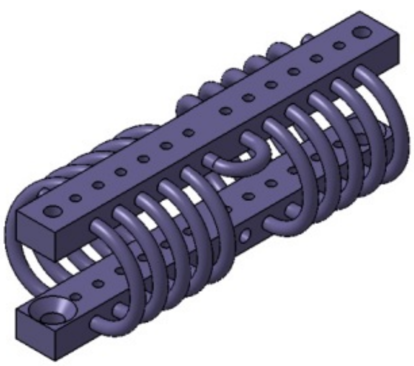
(a)

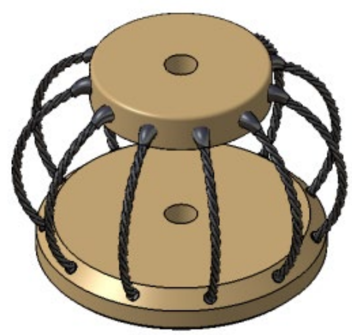
(b)

Fig.1. Helical Wire rope isolator (b) Polycal Wire rope isolator

The wire rope isolators mainly consist of two characteristics which enable it to be used as a vibration isolator and they are stiffness (K) and damping coefficient (C) [7]. The stiffness and damping coefficient defines the load-supporting and energy dissipation capabilities of the isolator respectively. The understanding of WRI requires the characterization of stiffness and damping coefficients through their monotonic and cyclic loading behavior respectively. The field of WRI is relatively new compared with other passive isolators hence only few research works are available and among the available research work, mostly are dedicated towards the cyclic loading behavior for damping coefficient. The major contributors for the behavior of WRI is presented. Tinker and Cutchins [5, 6] performed the experimental study for the damping phenomenon and suggested that the energy dissipation occurs through the friction between the individual wire strands.

Demetriades et *al.* [7] presented a study on the WRI using cylic loading. The study shows that WRI exhibits hysteresis curve under cylic loading and the hysteresis curve is symmetric for shear and roll load and asymmetric for tension/compression loading. They have deveopled mathematical model for hysterical behaviour using Bouc-Wen model and stated that WRI provides 10 % and 20-30% damping for large and small deformations respectively. The study also suggested that the asymmetric hysteresis curve during tension/compression is due to hardening and softening of the wire rope spring and suggested that the wire rope spring undergoes softening in compression and hardening in tension. The softening is due to the decrease in the contact points between the wire strands under compression load. The hardening in the tension is due to the increase in the contact points under tension load, which results in increased friciton between the wire strands [7] . Balaji et *al.*[8] performed the experimental study on the hysteresis behavior of WRI under cyclic loading in vertical and lateral direction and suggested that the wire rope diameter primarily influence the hysteresis behaviour

Massa et *al.* [9] introduced a ball bearing in the polycal WRI to increase its vertical stiffness. Ball bearing provides additional stiffness in the vertical direction to support the normal load of the equipment and hence increases the load carrying capacity. Paolacci and Giannini [10] conducted a study on the effectiveness of steel cable dampers for the seismic protection of electrical equipment. They developed a numerical model for an electrical equipment supported by WRI and subjected it to the sesmic load of the 1980 Irpinia earthquake (Italy). The study shows the effectiveness and potential of WRI as a base isolation system.

Endine Inc. [11] develops a series of vibration and shock isolators of many types and sizes including WRI and have provided the possible orientations of WRI that can be used in practical applications as shown in Fig.2. The orientation of the WRI depends mainly on the supporting structure to fix the WRI. In majority of the cases, the tension/compression loading mode is preferred. However based on the availability of the supporting structures, the WRI can also be used in the shear and the roll mode. Such orientation induces tension/compression, shear and roll load on the WRI as shown in Fig. 3 and the geometric properties of the WRI is shown in Fig. 4.

The procedure for the selection of WRI for a practical application is provided by Endine Inc [11] in their catalogue and it emphasis on the estimation of static stiffness, required by the WRI, based on the inputs such a static load, number and orientaiton of WRI, and input excitation frequency. Upon estimating the required static stiffness for 80% isolation, it is then required to select the WRI which possess that required stiffness in that required loading mode from the catalogue.

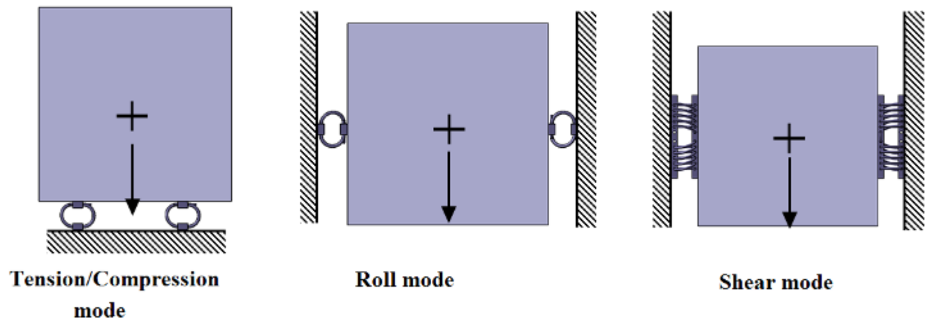

Fig.2. Orientations of WRI used in applications

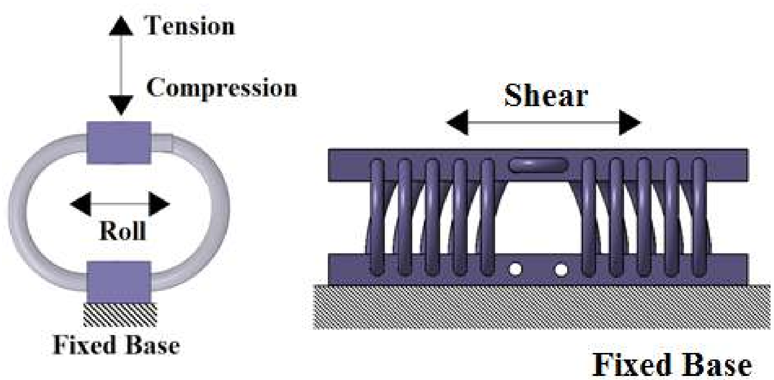

Fig.3. Loading of the WRI

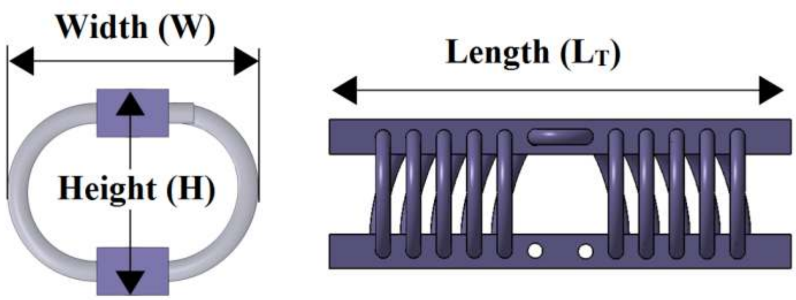

Fig.4. Geometeric characteristic of WRI

The Endine's catalogue [11] reports the geometric specifications and stiffness values of all the WRI in different loading modes. The stiffness values in the catalogue were determined using the experimental methods, as no analytical model is available in the literatures for the stiffness under different loading conditions. The major contribution on the static stiffness of the WRI is provided by Demetriades et al. [7]. The study showed that stiffness characteristics of the WRI depends on the diameter of the wire rope, width, height, length, number of turns and direction of load. The study using experimental tests on the WRI [7, 10] also concluded that the WRI exhibits the same behavior in vertical stiffness for both tension and compression load under small dispalcements. Pervious studies [7, 10] also suggested that stiff WRI provides better isolation. Hence it is required to provide the isolator with proper value of stiffness to achieve better isolation of the system.

The objective of the present work is to develop an analytical model of the stiffness for the helical WRI in the vertical directions under compressive load and validate it using monotonic loading tests. The analytical model is developed based on Castigliano's second theorm and the strain energy principles. The analytical model of the vertical stiffness is then used to perform a parameteric analysis to investigate the influence of wire rope diameter, width, height, and number of turns on the vertical compressive stiffness of WRIs.

2. Analytical work

The analytical model for the stiffness in the vertical direction is obtained by establishing a relationship between the displacement and the applied load. The input vibrational energy is absorbed by the WRI by undergoing a displacement and then release it through friction between the wire strands. Hence, the strain energy of the material and shape becomes a major factor in the design of the isolator. The Castigliano's second theorem [12] facilitates the relation between strain energy and displacement. The following assumptions were considered to simplify the analytical model:

1. The wire rope is considered as solid bar having uniform cross section;
2. The material of the wire rope is considered homogenous and isotropic;
3. The involvement of metal retainer in resisting the load is neglected;
4. The quastic static loading is considered;

5. The WRI is firmly mounted with no unwanted constraints.

2.1. Geometry of the WRI

The geometry of the WRI is simplified by considering a load carried by one coil of wire rope (Fig. 5 (a)). Furthermore, a single wire rope coil is symmetric about both vertical and horizontal axes, thus, one-quarter of the coil was considered in the model development (Fig. 6). The one-quarter coil, having a circular cross section of diameter D, can be divided into two regions. The first region is the top straight line of length L and the second region is the quarter circle of radius R (R=(H-T)/2). The boundary limits for each region are taken as; Region 1 : 0 to L and Region 2 : 0 to π/2; where the length L, is given by:

$$L = (W/2)-R-(D/2) \tag{1}$$

2.2. Analytical model of vertical stiffness

The deflection of a curved bar is usually calculated using Castigliano's theorem [13]. For the case of WRI, the cross section of the wire rope is small compared to the radius of curvature of its centerline. The compressive load and the reaction from the fixed base on a coil of WRI can be represented by two equal and opposite forces F as shown in Fig. 5 (b), where F is the load on a single coil of the WRI, which is given by P/N where P is the total load on the entire WRI and N is the number of turns (coils).

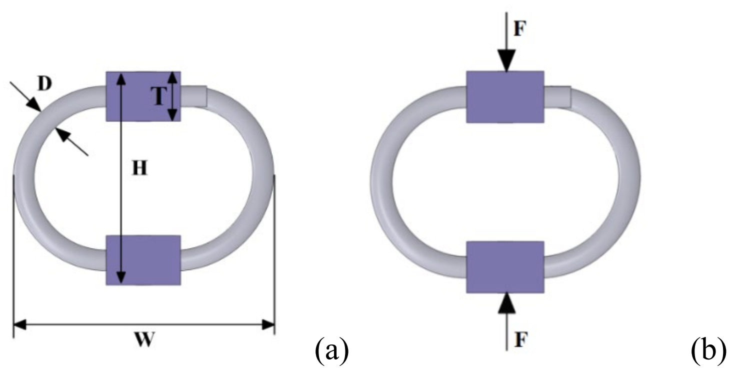

Fig.5. (a) Geometry of the WRI used in the analytical model (b) Load on the WRI

Due to the symmetry, only one quadrant of the coil is considered as shown in the Fig. 6. The shearing stress over the cross section is neglected and the compressive force on the cross section is given by F/2. The bending moment M_o, acting on the cross section is statically indeterminate and shall be determined using Castigliano's theorem. It can be seen from Fig. 5(b) that due to the condition of symmetry that the cross section does not rotate during bending of the wire rope. Hence the displacement due to M_o is zero, that is:

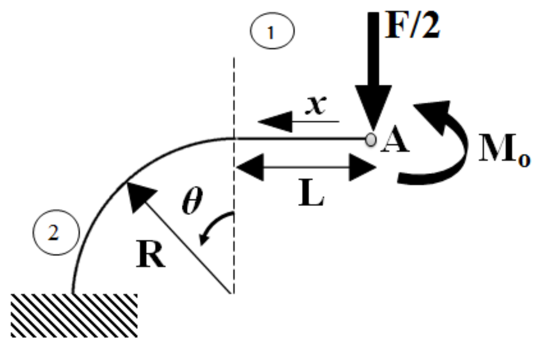

Fig.6. One-quarter coil of WRI under consideration

$$\frac{dU_1}{dM_o} = 0 \tag{2}$$

where U is the strain energy of the quadrant of the wire rope. The quadrant under consideration is sectioned into two regions (Fig. 6). Both regions undergo bending along their entire length. Whereas region 2 is in the form of a semicircular arc, hence it is integrated in radial coordinates. Hence, Eq.(2) can be written as:

$$\frac{1}{EI}\left[\int_0^L M_1 \frac{dM_1}{dM_o} dx + \int_0^{\frac{\pi}{2}} M_2 \frac{dM_2}{dM_o} R d\theta\right] = 0 \tag{3}$$

The bending moment in region 1 (M_1) and in region 2 (M_2) are given by:

For region 1:

$$M_1 = \frac{F}{2} x - M_o \tag{4}$$

and

$$\frac{dM_1}{dM_o} = -1 \tag{5}$$

For region 2:

$$M_2 = \frac{F}{2}(L + R\sin\theta) - M_o \tag{6}$$

and

$$\frac{dM_2}{dM_o} = -1 \tag{7}$$

Substituting Eqs. (4)-(7) into Eq.(3) yields:

$$\frac{1}{EI}\left[\int_0^L \left(\frac{F}{2}x - M_o\right)(-1)dx + \int_0^{\frac{\pi}{2}} \left(\frac{F}{2}(L + R\sin\theta) - M_o\right)(-1)Rd\theta\right] = 0 \tag{8}$$

Upon solving Eq.(8) for the statically indeterminant moment M_o we obtain:

$$M_o = \frac{FL^2 + \pi FLR + 2FR^2}{(4L + 2\pi R)} \tag{9}$$

The bending moment at any cross section of the wire rope can be calculated using Eq.(4) and Eq.(6) depending on the region. The total strain energy stored in the wire rope is given by:

$$U = 4 \times \frac{1}{2EI}\left[\int_0^L (M_1^2)dx + \int_0^{\frac{\pi}{2}} (M_2^2)Rd\theta\right] \tag{10}$$

and the deflection due to the applied load F, can be calculated using Catigliano's theorem:

$$\delta = \frac{dU}{dF} = 4 \times \int_0^L M_1 \frac{dM_1}{dF}dx + \int_0^{\frac{\pi}{2}} M_2 \frac{dM_2}{dF}Rd\theta \tag{11}$$

Substituting Eq.(4) and Eq.(6) into Eq.(11) gives the deflection due to the applied load F:

$$\delta = \frac{F(2L^4 + 4L^3R\pi + 24R^2L^2 + 6R^3L\pi + 3R^4\pi^2 - 24R^4)}{12EI(2L + R\pi)} \tag{12}$$

Finally, the vertical stiffness (K_v) of the complete WRI is calculated to be

$$K_V = \frac{dP}{d\delta} = N \times \frac{12EI(2L + R\pi)}{(2L^4 + 4L^3R\pi + 24R^2L^2 + 6R^3L\pi + 3R^4\pi^2 - 24R^4)} \tag{13}$$

The term EI, which is the product of the elastic modulus (E) and moment of inertia (I), in the analytical model (Eq.(13)), represents the resistance of the wire rope to bending and refered to as the flexural rigidity. Previous studies [14, 15] have reported a broad range of values of for the elastic modulus, ranging from 90 GPa to 200 GPa for various types and constructions of wire rope cables. The elastic modulus of the wire rope, in general, is load dependent [16]. Furthermore, the wire rope has a lower moment of inertia compared to the solid bar [15]. Previous studies have attempted to develop the analytical [17, 18] and numerical model [19, 20] of wire rope cables behaviour. However, these studies have dealt with the the straight, single, and multi stranded wire ropes under axial tensile loading. However, the wire rope of the WRI is patterned in a helical form and literatures lack the research work on the behavior of curved wire ropes under bending load and hence, it is obtained experimentally in the present work using the transverse bending test [16].

3. Experimental work

The present study reports two types of experiments: (1) monotonic loading test to validate the analytical model for the static vertical stiffness of WRIs, and (2) transverse bending test to estimate the flexural stiffness of the wire rope cable used to construct the WRI.

3.1. Montonic loading test

The static vertical stiffness of the WRI, which identifies the load carrying capacity, can be obtained from the behavior due to the unidirectional load in the vertical direction. The slope of the force-displacement plot provides the vertical stiffness of the WRI. Previous research [7, 10] have suggested that the WRI exhibits linear force-displacement curve for small displacements and becomes non-linear for higher displacement magnitudes. The monotonic loading test was performed using the GOTECH servo-hydraulic Computerized Universal Testing Machine (UTM) available in-house (Fig. 7). The UTM was configured to apply a compressive load at a slow rate of 0.1 mm/min to minimize the inertia effects and to achieve the quasi-static condition. The displacement applied and the corresponding load were recorded after every load step. The loading was performed only up to 5 mm displacement. The specifications of the WRIs used for the monotonic loading test is shown in Table.1. The WRI were made from 6×19 IWRC (Independent Wire Rope Core) stainless steel wire rope cables. The load-displacement plots are shown in Fig. 8. The obtained data points (displacement, force) were best fitted with the linear polynomial curve to obtain the slope, which is the static vertical stiffness of the WRI.

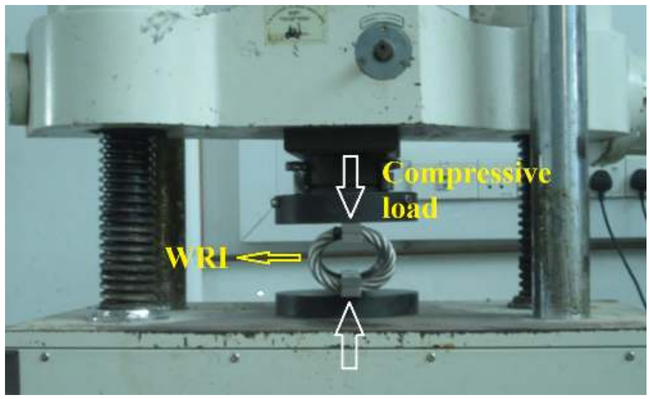

Fig.7. Compression test of WRI in the UTM

Table.1. Geometric characteristics of WRI used in the monotonic loading test

Isolator No.	Wire rope diameter (D) (mm)	Number of coils (N)	Width (W) (mm)	Height (H) (mm)	Length (L_T) (mm)	Thickness (T) (mm)
1	6.4	8	64	54	146	14
2	6.4	8	89	65	146	14
3	9.5	8	84	71	216	18
4	9.5	8	90	75	216	18
5	9.5	8	105	76	216	18
6	12	8	105	90	216	20
7	12	8	121	95	216	20
8	15.9	8	112	99	268	27

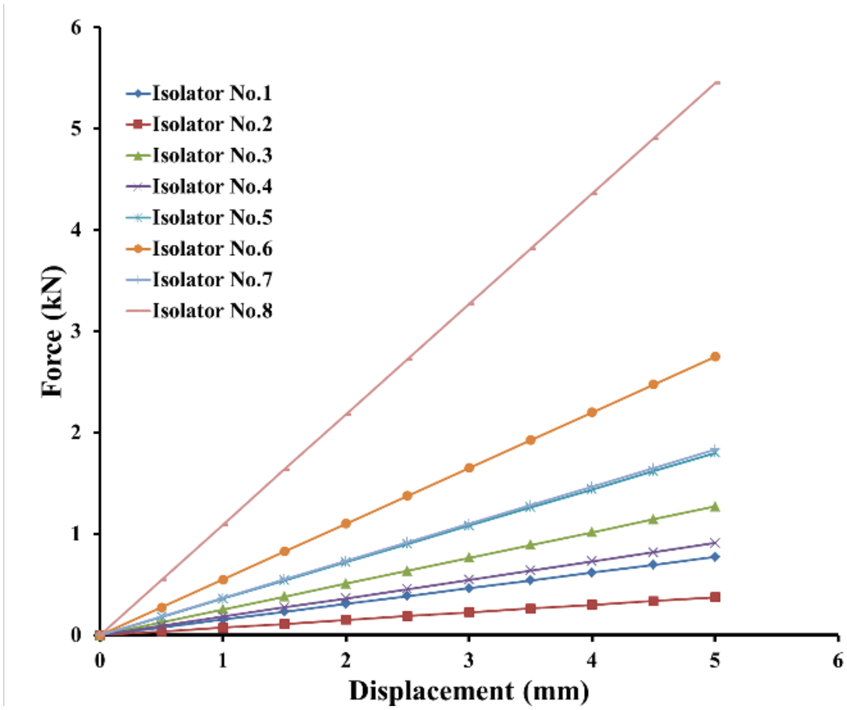

Fig.8. Load-Displacement plot for all the isolators under compressive load

3.2. Transverse bending test

The flexural rigidity of the wire rope cable depends on the material and specification of the wire rope cables [17]. Zhu and Meguid [16] has performed the transverse bending test for the 6×37 IWRC, steel cables and the present work followed the similar test procedure to obtain the flexural rigidity, EI, for the 6×19 IWRC stainless steel wire cables. ASTM A931-08 [21] was also referred to for the geometric characterization and selection of wire rope test samples. The wire ropes having diameters of 6.4 mm, 9.5 mm, 12 mm, and 15.9 mm were selected for the test. The flexural rigidity of the cantilever beam (Fig. 9) can be determined by using the end delfection due to the point load acting at the free end. The flexural rigidity can be expressed as:

$$EI = \frac{L_O^3}{3}\left(\frac{W}{Y}\right) \tag{14}$$

where W is the load acting at the free end, L_o is the beam's length, and Y is the free end deflection.

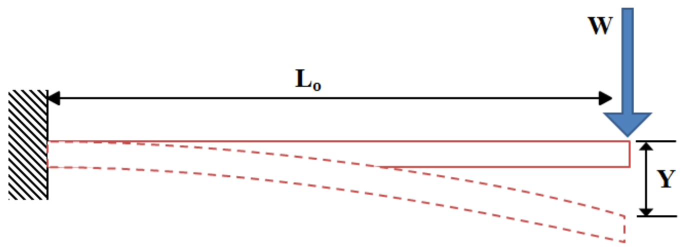

Fig.9. Cantilever with end load

The transverse force was applied at the end of the 300 mm length wire rope to measure its flexural rigidity (Fig. 10). The deflection was measured using the ABSOLUTE Digimatic Indicator, which features an accuracy of 0.02 mm and a resolution of 0.01 mm. Three samples of wire ropes were tested and the average deflection for each load increment is calculated to plot the load-displacement curve shown in Fig. 11. The slope (W/Y) was obtained from the best fit linear curve (W = slope x Y).

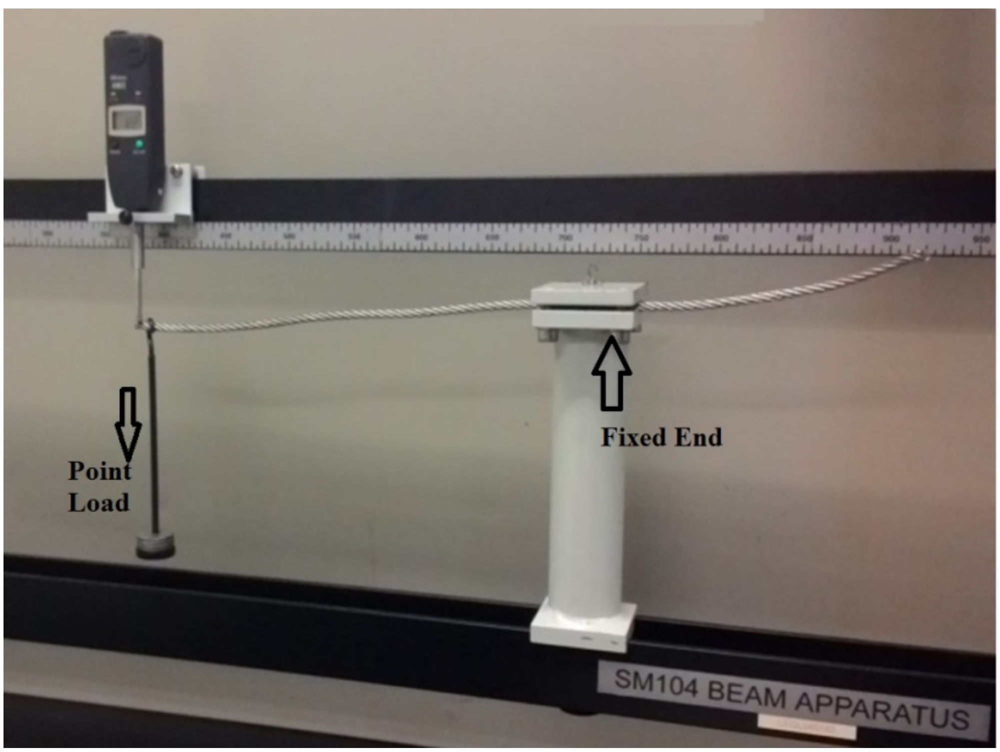

Fig.10. Experimental setup of the transverse bending test

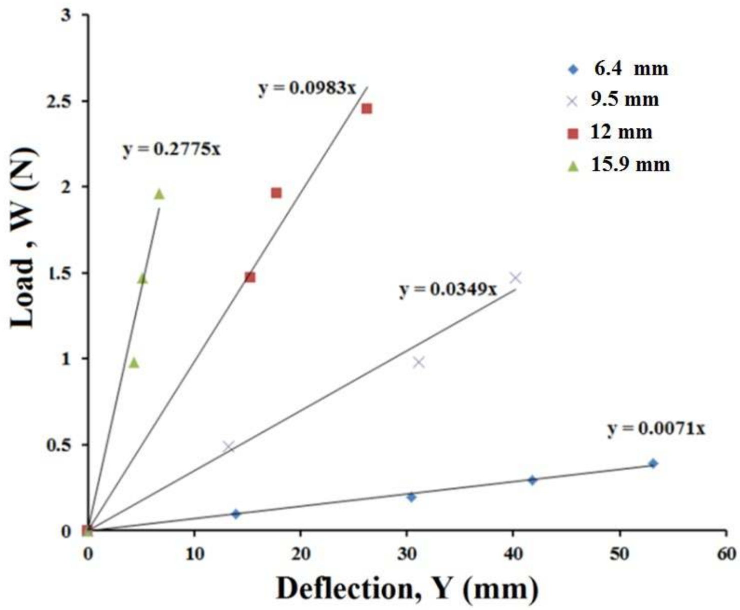

Fig.11. Force-Displacement plot from transverse bending tests

The slope obtained from the transverse bending tests (Fig. 11) were further substituted into Eq. (13) to obtain the EI of each wire rope. Table 2 summarized the variation of EI with the variation of wire rope diameters. The third order polynomial equation was found to best fit the data points (Fig. 12). This equation can be used to obtain EI for the 6×19 IWRC stainless steel wire cables. From Fig. 12, it is observed that the EI for the wire rope was found to increase cubicly with the wire rope diameter. This is attributed to the increased diameter of individual wires.

Table.2. Flexural rigidity of the 6x19 IWRC obtained from the transverse bending test.

Wire rope diameter (mm)	Slope (N/mm)	EI (N-mm^2)
6.5	0.0071	63900
9.4	0.0349	314100
12	0.0983	884700
15.9	0.2775	2497500

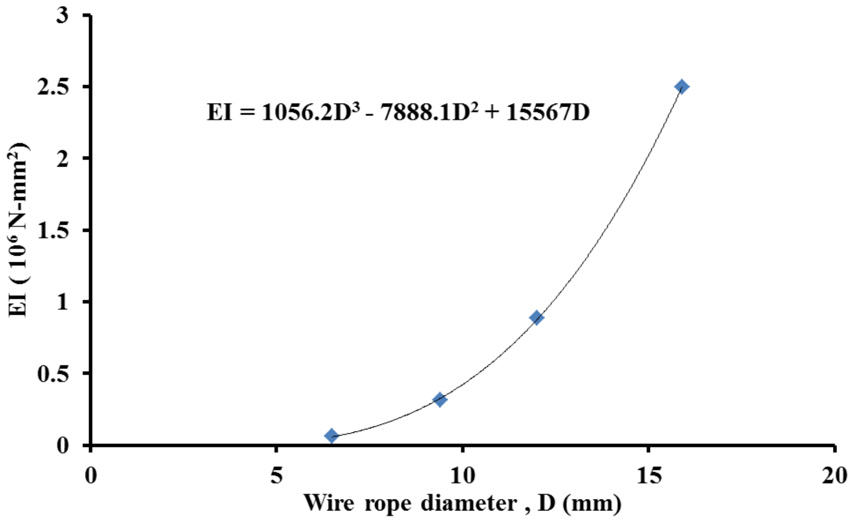

Fig.12. Variation of flexural rigidity (EI) with respect to wire rope diameter (6x19 IWRC)

4. Results and discussions

The analytical model represented by Eq. (13) is validated using the monotonic test results. The flexural rigidity required in the analytical model is obtained from the transverse bending test (Table. 2). The monotonic loading results for various WRI is shown in Fig. 8. The comparison between the analytical and the experimental test results is shown Fig. 13 and tabulated in Table 3. It is observed that, the analytical model has a good agreement with the experimental results within 10% deviation. The analytical model provides the vertical stiffness in terms of the geometric properties and hence, extended for an analytical study. Another major application of the analytical model is that its ability to be used for the design of the WRI to obtain the desired vertical stiffness. The present analytical model also can be evaluated for the modification required in the geometric properties to obtain the required increase in stiffness.

Table.3. Comparison of analytical and experimental vertical stiffness

Isolator No.	K_v (Experimental), N/mm	K_v (Eq.(13)), N/mm	Error (%)
1	154.6	156.58	1.28
2	74.8	81.69	9.21
3	254	280.81	10.55
4	182	174.13	4.32

5	360	354.89	1.42
6	550	520.23	5.41
7	367	345.55	5.84
8	1090	1110.23	1.86

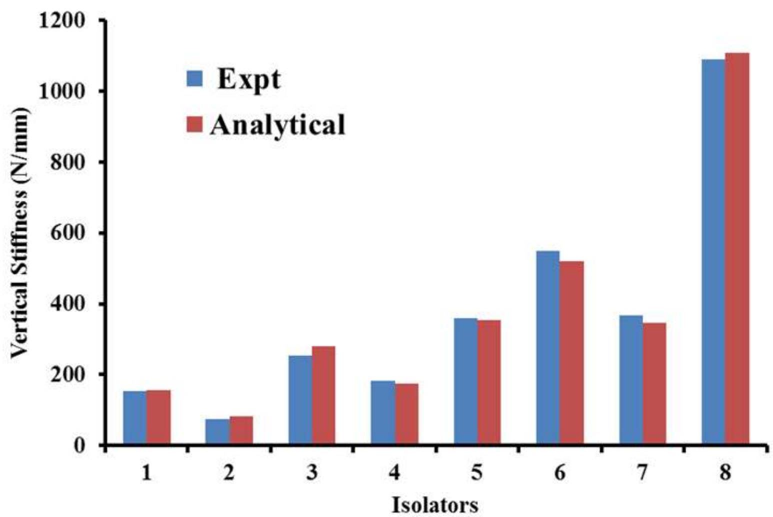

Fig.13. Experimental and analytical WRI's vertical stiffness

4.1. Influence of wire rope diameter

WRI is made up of wire rope cables, hence its diameter has a significant effect on the behavior of WRI. The quantified effects of wire rope diameter on the stiffness of WRI are not reported in the literature. Thus, it would be interesting to observe the wire rope diameter effects on stiffness. The effects of wire rope diameter (D) on the vertical stiffness is shown in Fig. 14 for various values of number of turns (N). It is observed from the analytical model (Eq. (13)) that the vertical stiffness is highly dependent on the wire rope diameter, or in other words, one of the effective ways to control the stiffness is to adjust the wire rope diameter. The significant increase in the vertical stiffness is due to the increase of flexural rigidity, EI, which in turn increases with wire rope diameter. Increasing the diameter from 6.4 mm to 15.9 mm induces an increase of the vertical stiffness by a factor of $(15.9/6.4)^4$ ~38.1. Evidently, increasing the number of turns would increase the stiffness; this relationship is linear as evidenced by Eq. (13).

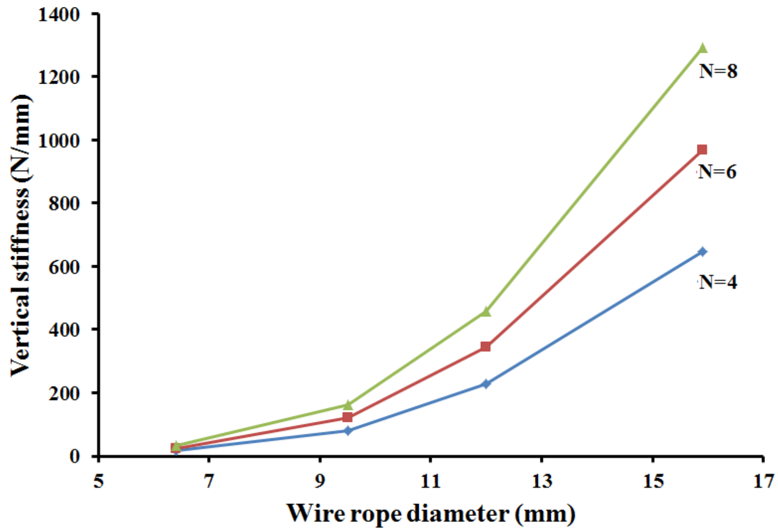

Fig.14. Variation of vertical stiffness with wire rope diameter of the WRI with different number of turns, N.

4.2. Influence of Width and Height

The width and height of the WRI control the geometry of the coil, hence affecting the stiffness from a geometrical perspective (L and R in Eq.(13)). An increase in width with constant height results in a decrease of vertical stiffness (Fig. 15(a)). Similarly, an increase in height with constant width results in a decrease of vertical stiffness (Fig. 15(b)). However, the height-to-width ratio would be an interesting parameter to study its influence on the effect on the vertical stiffness. Fig. 16 shows the variation of the height to width ratio for various wire rope diameters. It can be seen that by increasing the ratio from 0.6 to 1.2, the stiffness increases, which is significant for higher wire rope diameters. The effect of height-to-width ratio on the vertical stiffness is less pronounced for small wire rope diameters. For higher values of height-to-width ratio, the stability of the coil in the lateral direction decreases and the lateral restoring force of the WRI is reduced affecting the isolator's performance. Hence, the present trend in the industry is majorly to maintain a ratio of 0.75–0.85 for a stable wire rope isolator. From the monotonic tests, it can be seen that isolator 5 and 7 have similar stiffness, however, they were made from different wire rope diameters, which can be explained by the differences in width and height. The width and height can be controlled to obtain an higher vertical stiffenss from the lower diameter wire rope, however, the height-to-width ratio has to maintained within the limits of 0.75-0.85.

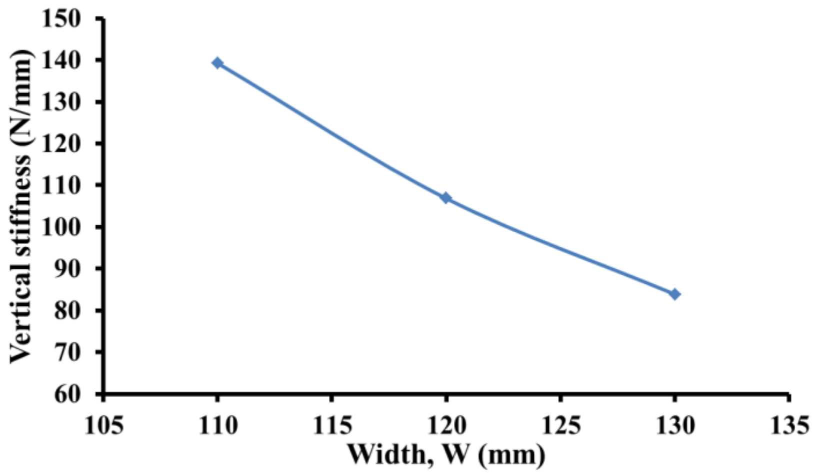

(a)

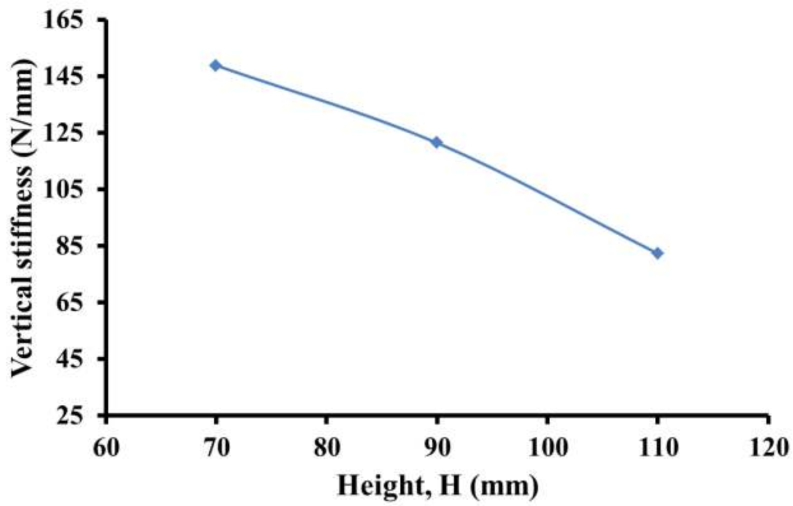

(b)

Fig.15. Variation of stiffness (a) Width (b) Height

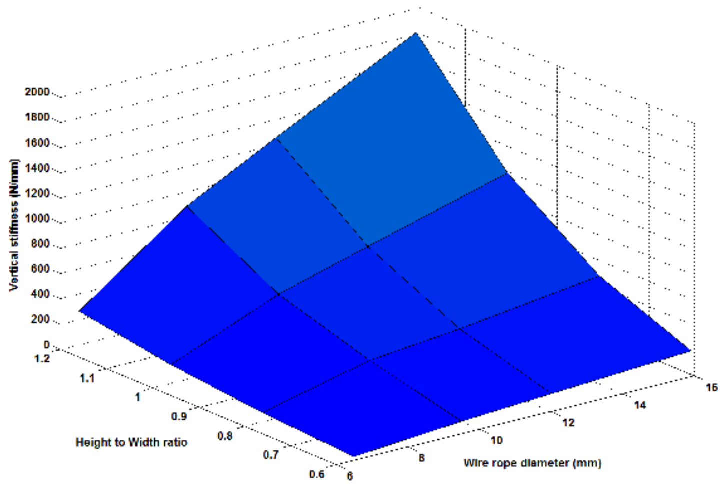

Fig.16. Variation of vertical stiffness with height-to-width ratio and wire rope diameter

4.3. Influence of Number of turns

The Number of turns provides the additional wire loops to support the weight of the equipment. From Eq.(13), it is clear that the vertical stiffness is directly proportional to the number of turns. From a stability point of view, a stiffer WRI should be designed to have a sufficient number of turns with a small wire rope diameter rather than a small number of turns with greater wire rope diameter. Generally, manufacturers opt for 8-turns WRIs.

5. Conclusion

In this work we presented an analytical model for the vertical stiffness of wire rope isolators. The model was validated with experimental data obtained from a series of monotonic loading tests. The developed model can be effectively used to evaluate and design of wire rope isolators. The following conclusion can be drawn form the present work.

1. The transverse bending test was used to estimate the flexural rigidity, EI, of the 6x19 IWRC wire rope cables. A simple equation was developed to estimate the EI for similar wire ropes with different diameters.
2. The vertical stiffness is linearly proportional to the. number of turns
3. The wire rope diameter significantly influences the vertical stiffness more than the width, height, and number of turns.
4. An increase in wire rope diameter increases the vertical stiffness, however, increase of either width or height results in the decrease in vertical stiffness.

5. A 10% increase vertical stiffness can be achieved either by increasing the wire rope diameter by 2.5% or decreasing the width by 3.3 %.

Acknowledgment

This paper is based upon work supported by both the Ministry of Higher Education (MOHE), Malaysia under the ERGS grant scheme and the University of Sharjah through the SEED funding scheme.

References

[1] J. Alanoly, S. Sankar, A New Concept in Semi-Active Vibration Isolation, Journal of Mechanical Design, 109 (1987) 242-247.

[2] R.A. Ibrahim, Recent advances in nonlinear passive vibration isolators, Journal of Sound and Vibration, 314 (2008) 371-452.

[3] M. Ismail, J. Rodellar, F. Ikhouane, Seismic protection of low- to moderate-mass buildings using RNC isolator, Structural Control and Health Monitoring, 19 (2012) 22-42.

[4] E.I. Rivin, Passive Vibration Isolation, (Professional Engineering Publishing, 2003).

[5] T. Michael Loyd, Damping Phenomena in a Wire Rope Vibration Isolation System, Doctor of Philosophy, Aerospace Engineering, Auburn University, 1989.

[6] M.L. Tinker, M.A. Cutchins, Damping phenomena in a wire rope vibration isolation system, Journal of Sound and Vibration, 157 (1992) 7-18.

[7] G.F. Demetriades, M.C. Constantinou, A.M. Reinhorn, Study of wire rope systems for seismic protection of equipment in buildings, Engineering Structures, 15 (1993) 321-334.

[8] P.S. Balaji, Leblouba Moussa, M.E. Rahman, L.T. Vuia, Experimental investigation on the hysteresis behavior of the wire rope isolators, Journal of Mechanical Science and Technology, Accepted for Publications (2015).

[9] G. Massa, S. Pagano, E. Rocca, S. Strano, Sensitive equipments on WRS-BTU isolators, Meccanica, 48 (2013) 1777-1790.

[10] P. Paolacci, R. Giannini, Study of The Effectiveness of Steel Cable Dampers For The Seismic Protection of Electrical Equipment, in: The 14th World Conference on Earthquake Engineering. Beijing, China, 2008).

[11] Wire rope Isolators, ITT Enidine Inc, New York, www.enidine.com, (2014).

[12] R.G. Budynas, J.K. Nisbett, J.E. Shigley, Shigley's mechanical engineering design, (McGraw-Hill, 2008).

[13] S. Timoshenko, Strength of Materials, Pt. 2: Advanced Theory and Problems, (R. E. Krieger Publishing Company, 1983).

[14] R.P. Kusy, G.J. Dilley, Materials Science Elastic Modulus of a Triple-stranded Stainless Steel Arch Wire via Three- and Four-point Bending, Journal of Dental Research, 63 (1984) 1232-1240.

[15] Y. Prawoto, R.B. Mazlan, Wire ropes: Computational, mechanical, and metallurgical properties under tension loading, Computational Materials Science, 56 (2012) 174-178.

[16] Z.H. Zhu, S.A. Meguid, Nonlinear FE-based investigation of flexural damping of slacking wire cables, International Journal of Solids and Structures, 44 (2007) 5122-5132.

[17] G.A. Costello, G.J. Butson, Simplified Bending Theory for Wire Rope, Journal of the Engineering Mechanics Division, 108 (1982) 219-227.

[18] S. Baragetti, A Theoretical Study on Nonlinear Bending of Wires, Meccanica, 41 (2006) 443-458.

[19] E. Stanova, G. Fedorko, M. Fabian, S. Kmet, Computer modelling of wire strands and ropes Part I: Theory and computer implementation, Advances in Engineering Software, 42 (2011) 305-315.

[20] E. Stanova, G. Fedorko, M. Fabian, S. Kmet, Computer modelling of wire strands and ropes part II: Finite element-based applications, Advances in Engineering Software, 42 (2011) 322-331.

[21] ASTM A931- 08 (Reapproved 2013) Standard test method for tension testing of wire ropes and strand, in.).